Two new species of *Hornibrookina* Edwards, 1973 from the Austral Basin, Patagonia: Biostratigraphical and palaeoecological implications

Juan P. Pérez Panera*

CONICET–YPF Tecnología, Av. del Petróleo s/n, 1923 Berisso, Buenos Aires, Argentina; perezpanera@gmail.com

Diana I. Ronchi

GEMA SRL – YPF Tecnología, Av. del Petróleo s/n, 1923 Berisso, Buenos Aires, Argentina; sianaronchi@gmail.com

Abstract Two new species of the genus *Hornibrookina*—*H. larae* sp. nov. and *H. nicolasii* sp. nov.—are described and illustrated. These species were first reported from surface and subsurface Early to Middle Eocene sedimentary successions in the Austral Basin, Patagonia, Argentina. Accompanying calcareous nannofossils and foraminifera from an outcrop sample from the Río de la Turba area, where these new species are well preserved and abundant, are discussed to better constrain the age and palaeoecology of the new species. These new species extend the geological range of the genus *Hornibrookina* into the Late Lutetian–Early Bartonian (NP16) and support its affinity for coastal, eutrophic marine conditions.

Keywords *Hornibrookina larae*, *Hornibrookina nicolasii*, Middle Eocene, biostratigraphy, palaeoecology, South Atlantic Ocean

1. Introduction

Biostratigraphical investigations conducted by oil industry personnel in the Austral Basin, Patagonia, Argentina revealed the presence of two new species of *Hornibrookina* Edwards, 1973. These species had been previously documented from cuttings of Early to Middle Eocene subsurface successions from different parts of the Austral Basin. Recently, they were both recorded in a moderately to well-preserved assemblage of calcareous nannofossils from a Middle Eocene outcrop in the Isla Grande de Tierra del Fuego, Argentina (Figure 1). In this material, the stratigraphical uncertainties associated with cuttings were avoided, and planktonic and benthic foraminifera were able to provide additional age constraints for these new species. The purpose of this contribution is to describe and illustrate these new species and to highlight what this discovery means regarding the evolution and palaeoecology of the genus *Hornibrookina*.

2. Geological background

The Austral Basin lies in southern South America and spans part of Patagonia and the
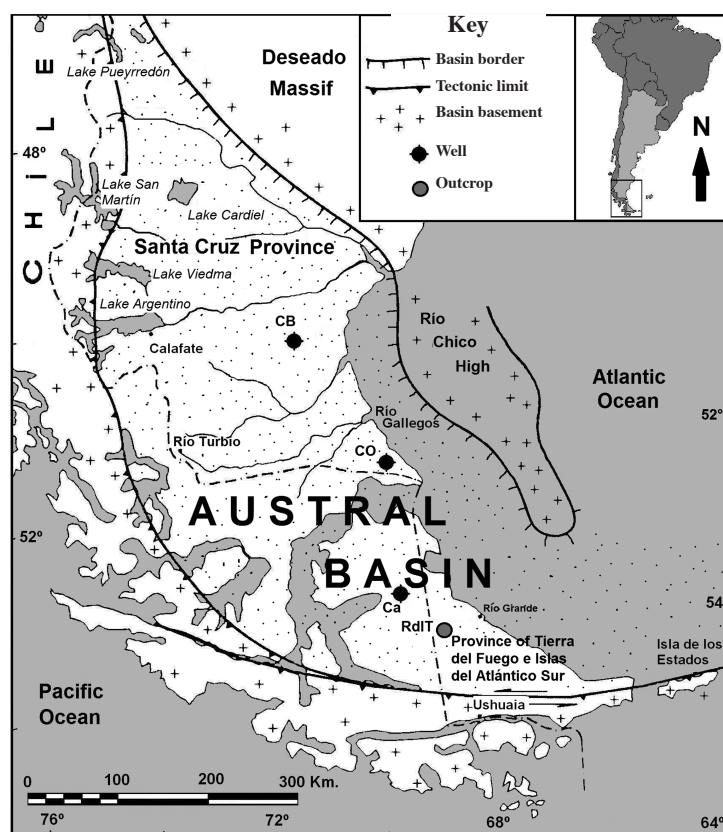
Figure 1: Map of southern Patagonia showing the extent of the Austral Basin (dotted area) and the locations of the mentioned sites. Modified after Nullo et al. (1999). **CB**—Campo Bola Well, **CO**—Cóndor Oeste Well, **Ca**—Carpintero Well, **RdlT**—Río de la Turba outcrop

Argentinian Continental Shelf, including the Isla Grande de Tierra del Fuego (Figure 1). It developed between the Andean Cordillera to the west and the Rio Chico High on the Patagonian Shelf to the east (Malumián, 1999; Nullo et al., 1999). Together with the adjacent, offshore Malvinas Basin, it formed near a complex tectonic area, which was greatly affected by interaction between the South American, Scotia and Antarctic Plates (Galeazzi, 1998). Sedimentary infilling of the basin started in the Late Jurassic, and was triggered by the extensional tectonics that fragmented Gondwana and caused the early opening of the South Atlantic Ocean (Peroni et al., 2002). The Late Jurassic to Miocene sediments in this basin are predominantly marine and have a maximum thickness of up to 7000 m (Galeazzi, 1998). During the Late Cretaceous, the Austral Basin transformed into a foreland basin that accumulated the mainly fine-grained sediments of the *Inoceramus* beds (Olivero & Malumián, 2008; Sachse et al., 2015). From the Maastrichtian, the basin was subjected to changing sea levels, with the main Atlantic transgressions occurring during the Maastrichtian–Danian, the Middle Eocene, the Late Oligocene–Early Miocene and the Middle Miocene (Malumián & Náñez, 2011; Pérez Panera, 2013). The Palaeogene sedimentary cycles have distinctly different facies in different parts of the basin (Malumián, 1999, 2002; Olivero & Malumián, 2008). During this time, the deepest areas were in the south-eastern sector, near the Isla Grande de Tierra del Fuego and the Argentinian Continental Shelf. Sediments in the central and western parts of the basin were deposited in shallow-marine to continental environments.

3. Materials and methods

Cuttings samples from three industry wells (Carpintero, Chile, Cóndor Oeste and Campo Bola, Argentina) and one outcrop sample, (022) from the Río de la Turba outcrop preserving the La Despedida Group, were prepared for nannofossil analysis using the gravity settling technique of Bramlette & Sullivan (1961). The slides were scanned at 1000x magnification under polarised light using a Leica DM 2700P microscope, whilst a Leica DFC 295 digital camera was used to take photographs. Samples for scanning electron microscope (SEM) analysis were prepared from the Río de la Turba outcrop using a vacuum pump for filtration onto a 0.45-μm-pore, 47-mm-diameter Millipore filter, with the addition of a few drops of a commer-

cial glass-cleaning product to disperse the clays. An FEI Quanta 200 SEM was used to take photographs.

For the foraminiferal analysis, 20 g of washed rock was placed into a beaker to which 500 ml of water and 50 ml of 100-volume hydrogen peroxide were added. The sample was then boiled for 30 min to facilitate disaggregation. The material was washed under running water through a 74-μm-mesh sieve (200 Tyler Screen System) and dried in a sand bath. Five grammes of sediment were extracted from the residue for analysis. The foraminifera were picked and arranged onto slides for identification. The samples are stored in the YPF Tecnología SA Micropaleontological Repository (with the prefix YT.RMP_#) and the Facultad de Ciencias Exactas y Naturales of the Universidad Nacional de Buenos Aires micropalaeontological collection (with the prefix BAFC–NP).

4. Micropalaeontological results from the Río de la Turba outcrop

A moderately to well-preserved calcareous nannofossil assemblage was recovered from Sample 022 (Table 1), in which a total of 23 taxa were identified. The most abundant species—*Reticulofenestra minuta*—had a relative abundance of >50%, while the second most abundant species—*Hornibrookina larae* sp. nov.—represented 17.5%. The other relevant taxa were *Hornibrookina nicolasii* sp. nov., *Reticulofenestra daviesii*, *R. lockeri*, *R. reticulata*, small specimens of *R. bisecta*, *R. dictyoda*, *Cyclicargolithus floridanus*, *Toweius callosus*, *T. rotundus*, *Pontosphaera pygmaea*, *P. pulchra*, *Clausicoccus fenestratus*, *C. subdistichus* and *Sphenolithus predistentus*, among others (Table 1).

The benthic and planktonic foraminifera were moderately preserved, with the species richness and diversity being high among the benthics (Table 2). The most abundant benthic taxa were *Martinotiella communis*, *Spiroplectammina elgansoensis*, *S. spectabilis* (agglutinated forms) and *Anomalinoides pinguiglabra*, *Bulimina* sp., *Cibicides wuellerstorfi*, other unidentified *Cibicides* spp., *Cribrorotalia* spp., *Globocassidulina subglobosa*, *Gyroidinoides* ex gr. *zelandica*, *Heterolepa perlucida*, *Lenticulina alatolimbata*, *Uvigerina peregrina* and *Virgulinella severini* (calcareous forms). The planktonic foraminifera were moderately abundant, but most could not be identified to species level due to poor preservation. The only recognisable species were *Globigerinatheka index*, *Catapsydrax*

Table 1: Nannofossils recovered from Sample 022, Río de la Turba, La Despedida Group, Austral Basin, Isla Grande de Tierra del Fuego, Argentina

SAMPLE	FIELDS OF VIEW (FOVs) COUNTED	PRESERVATION	ABUNDANCE (nannofossils * FOV)	Blackites spinosus	Clausicoccus fenestratus	Clausicoccus subdistichus	Coccolithus pelagicus	Cyclicargolithus floridanus	Cyclicargolithus floridanus (small)	Hornibrookina larae sp. nov.	Hornibrookina nicolasii sp. nov.	Lithostromation simplex	Pontosphaera pulchra	Pontosphaera pygmaea	Pontosphaera sp. indet.	Pyrocyclus sp. indet.	Reticulofenestra bisecta (small)	Reticulofenestra daviesii	Reticulofenestra lockerii	Reticulofenestra minuta	Reticulofenestra reticulata	Reticulofenestra dictyoda (small)	Sphenolithus predistentus	Toweius callosus	Toweius sp. (small)	Umbilicosphaera jordanii	TOTAL SPECIMENS	SPECIES RICHNESS
022	~400	M/G	~0.75	1	2	1	3	2	12	53	14	1	3	5	1	1	5	15	3	158	4	8	1	2	4	1	300	23

Table 2: Foraminifera recovered from Sample 022, Río de la Turba, La Despedida Group, Austral Basin, Isla Grande de Tierra del Fuego, Argentina. P—porcellaneous

SAMPLE	PRESERVATION	Agglutinated									Calcareous																																		P	Planktonics					TOTAL SPECIMENS	SPECIES RICHNESS
		Ammodiscus sp.	Karreriella sp.	Martinotiella communis	Siphotextularia concava	Siphotextularia sp.	Spiroplectammina elgansoensis	Spiroplectammina roemeri	Spiroplectammina sp.	Spiroplectammina spectabilis	Alabamina atlantisae	Anomalinoides pinguiglabra	Astacolus spp.	Bolivina sp.	Bulimina sp.	Cibicides spp.	Cibicides ungerianus	Cibicides wuellerstorfi	Conolagena argentina	Cribrorotalia spp.	Dentalina cooperensis	Dentalina cf. tenuicostata	Eoguttulina anglica	Fursenkoina pontoni	Glabratella crassa	Globocassidulina subglobosa	Guttulina communis	Gyroidina neosoldanii	Gyroidinoides ex gr. zelandica	Heterolepa perlucida	Lagena substriata	Lenticulina alatolimbata	Lenticulina spp.	Lotostomoides asperula	Marginulina ex gr. hochstetteri form costulata	Marginulina sp. 2290 of Malumián (1990)	Marginulina sp.	Marginulinopsis asperuliformis	Neugeborina longiscata	Nodosaria latejugata	Oridorsalis sp.	Pullenia bulloides	Uvigerina peregrina	Virgulinella severini	Quinqueloculina seminula	Catapsydrax unicavus	Globigerinatheka index	Subbotina angiporoides	Indet. planktonics		
022	M	1	2	21	1	1	12	2	1	13	1	99	6	1	3	70	30	34	6	11	2	7	1	2	1	14	5	2	48	20	1	14	6	6	7	1	1	1	5	4	8	6	68	60	1	1	5	1	14	627	48

unicavus and *Subbotina angiporoides* (Table 2). The age of the Río de la Turba outcrop is Middle Eocene, based on a combination of calcareous nannofossil and foraminifera biostratigraphy.

5. Systematic palaeontology

Order **ISOCHRYSIDALES** Pascher, 1910
Family **PRINSIACEAE** Hay & Mohler, 1967 emend.
Young & Bown, 1997

Genus *Hornibrookina* Edwards, 1973
Type species *Hornibrookina teuriensis* Edwards, 1973

Diagnosis: Narrowly elliptical placoliths with a central-area filled by large bars. The proximal shield is mono-cyclic. The distal shield is bicyclic, with the inner cycle forming a crown-like structure (Young & Bown, 1997).

Hornibrookina larae Pérez Panera sp. nov.
Pl. 1, figs 1–9; Pl. 2, figs 1–16

2013 *Hornibrookina weimerae* Self-Trail, 2011: Pérez Panera, pp. 129–130.
Derivation of name: Named in honour of Lara Pérez Panera, daughter of Juan P. Pérez Panera. **Diagnosis**: Small

Hornibrookina with eight to nine parallel pairs of laths in the central-area and one cycle of elements in the proximal shield. **Description**: Small, elliptical placolith with a medium to large central-area occupied by eight to nine pairs of laths that are aligned perpendicular to the major axis of the ellipse. Each pair of laths meets at the centre and their ends may be enlarged. There is no longitudinal bar. The distal shield is composed of two cycles of elements. In the inner cycle, the elements are high and slightly imbricated clockwise in distal view. The outer cycle is thin, flat and has low birefringence in cross-polarised light. The proximal shield is composed of only one cycle of elements, to which the eight or nine pairs of laths are attached. The elements of the distal and proximal shields become detached from each other as they approach the rim of the placolith, producing a spinose or serrated outline, but this could be due to dissolution. Under crossed polarisers, the tube is highly birefringent and the outline of the coccolith appears weakly serrated; the central-area is always dark. **Differentiation**: *Hornibrookina larae* differs from *H. weimerae* in being slightly larger and wider, and by having thin laths, rather than flat, overlapping laths, in the central-area. This species is difficult to distinguish with the light-microscope (LM), but the central-area in *H. larae* is dark and the coccolith outline is slightly serrated, whereas, in *H. weimerae*,

the central-area is poorly birefringent and the coccolith outline is smooth. *Hornibrookina larae* differs from *H. nicolasii* in its smaller size, relatively thinner distal shield, monocyclic proximal shield, and the different number and arrangement of the laths. **Remarks**: Most of the SEM illustrations of the specimens in Plate 1 show strong dissolution and are poorly preserved. Dissolution most likely occurred during preparation of the SEM sample. The addition of the glass-cleaner product to the sample worked perfectly in eliminating the clay, but may have affected the delicate, small nannofossils, such as *H. larae*. However, these specimens are still useful for determining the number and arrangement of the laths in the central-area and the nature of the distal and proximal shields. **Dimensions**: Length = 2.33–3.50 μm; width = 1.40–2.50 μm; axial ratio = 1.36–2.00 (Table 3). **Holotype**: YT.RMP_N.000007.2-1 (Pl. 1, fig. 1). **Paratypes**: YT.RMP_N.000007.2-2 (Pl. 1, fig. 2), YT.RMP_N.000007.2-3 (Pl. 1, fig. 3), YT.RMP_N.000007.2-4 (Pl. 1, fig. 4), YT.RMP_N.000007.2-5 (Pl. 1, fig. 5), YT.RMP_N.000007.2-6 (Pl. 1, fig. 6), YT.RMP_N.000007.2-7 (Pl. 1, fig. 7), YT.RMP_N.000007.2-8 (Pl. 1, fig. 8), YT.RMP_N.000007.2-9 (Pl. 1, fig. 9), YT.RMP_N.000007.1-1 (Pl. 2, fig. 1), YT.RMP_N.000007.1-2 (Pl. 2, figs 2–5), BAFC-NP 3397-1 (Pl. 2, fig. 6), BAFC-NP 3397-2 (Pl. 2, fig. 7), BAFC-NP 3397-3 (Pl. 2, fig. 8), YT.RMP_N.000009.1-1 (Pl. 2, fig. 9), YT.RMP_N.000009.1-2 (Pl. 2, figs 10–12), YT.RMP_N.000009.1-3 (Pl. 2, fig. 13), YT.RMP_N.000009.1-4 (Pl. 2, fig. 14), BAFC-NP 3397-4 (Pl. 2, fig. 15), BAFC-NP 3397-5 (Pl. 2, fig. 16). **Type locality**: Río de la Turba section, Argentina (53.92°S, 68.38°W). **Type level**: Sample 022, La Despedida Group, NP16, Middle Eocene. **Occurrence**: Early to Middle Eocene (NP13–NP16) in the Austral Basin, Patagonia. Ypresian in the Carpintero Well (1300–1310 m depth); Late Ypresian to Early Bartonian (NP13–NP16) in the Campo Bola Well (1025–1030 to 1015–1020 m); Lutetian to Early Bartonian (NP15–NP16) in the Cóndor Oeste Well (1065–1105 m); Late Lutetian to Early Bartonian (NP16) in the Río de la Turba outcrop.

Hornibrookina nicolasii Pérez Panera sp. nov.
Pl. 3, figs 1–9; Pl. 4, figs 1–30

Derivation of name: Named in honour of Nicolás Pérez Panera, son of Juan P. Pérez Panera. **Diagnosis**: A medium-sized species of *Hornibrookina* with a broad, bicyclic distal shield, broad, monocyclic proximal shield and central-area filled by 11 to 14 pairs of alternating laths. **Description**: Medium-sized, elliptical placolith with a broad, bicyclic distal shield and a medium to large central-area occupied by 11 to 14 flattened pairs of laths that are perpendicular to the inner wall of the shield. The junction of the laths is slightly offset and forms parallel to the major axis of the ellipse. Overgrowth can result in enlarged ends on the laths, which form a 'hammer' shape. There is no separate longitudinal bar. The outer cycle of the distal shield is broad and the elements are slightly imbricated clockwise in distal view. The elements have a trapezoidal shape and are thinner towards the central-area. This produces a conspicuous slit between the elements that is also distinctive in the LM. The inner cycle of the distal shield is tall and thin. In some specimens, protruding knobs have developed at the contact between the outer and inner cycles of the distal shield. The proximal shield is also broad, but smaller than the distal shield. Under crossed polars, the inner cycle of the distal shield is highly birefringent, while the outer cycle has low birefringence and a serrated aspect due to the thinning of the elements between the sutures. The central-area has low birefringence and, in some cases, a bright line appears subparallel to the major axis of the ellipse. This is due to the enlargement of the laths where they connect and not because of the presence of a longitudinal bar. **Differentiation**: *Hornibrookina nicolasii* differs from other species of the genus in having an outer cycle of elements with slits between them, which gives a spinose aspect under crossed polarisers. It also differs from the co-occurring *H. larae* in its larger size and different arrangement of laths. **Remarks**: When observed under crossed polarisers and with a gypsum plate, the tube and distal shield elements show the same crystallographic orientation (Pl. 4, figs 10, 14). This is not the case in other species of *Hornibrookina*, where the tube elements correspond to R-units and the shield elements to V-units, producing an alternation of colours between the tube and the distal shield. However, it is possible that the birefringent elements correspond to the proximal shield elements that

Table 3: *Hornibrookina larae* and *H. nicolasii* measurements from SEM specimens

Hornibrookina larae SEM SPECIMENS	VIEW	# LATHS	LENGTH	WIDTH	ELLIPTICITY (L/W)
YT.RMP_N.000007.2-1	distal	9	3.5	2.5	1.40
YT.RMP_N.000007.2-2	distal	9	3	1.83	1.64
YT.RMP_N.000007.2-3	proximal	8	3.1	1.55	2.00
YT.RMP_N.000007.2-4	distal	8	3	2.2	1.36
YT.RMP_N.000007.2-5	distal	9	3.33	2	1.67
YT.RMP_N.000007.2-6	distal	8	2.33	1.5	1.55
YT.RMP_N.000007.2-7	proximal	8	2.73	1.95	1.40
YT.RMP_N.000007.2-8	proximal	8?	2.63	1.9	1.38
YT.RMP_N.000007.2-9	distal	8	2.64	1.7	1.55
YT.RMP_N.000007.2-18	distal	8?	2.42	1.4	1.73
Hornibrookina nicolasii SEM SPECIMENS	VIEW	# LATHS	LENGTH	WIDTH	ELLIPTICITY (L/W)
YT.RMP_N.000007.2-10	distal	13	6	4	1.50
YT.RMP_N.000007.2-11	distal	10–11	6	3.84	1.56
YT.RMP_N.000007.2-12	distal	?	5.48	4.08	1.34
YT.RMP_N.000007.2-13	distal	11	5.66	4.13	1.37
YT.RMP_N.000007.2-14	distal	11	5.7	3.66	1.56
YT.RMP_N.000007.2-15	distal	11–12	5.63	3.81	1.48
YT.RMP_N.000007.2-16	proximal	11	5.66	3.66	1.55
YT.RMP_N.000007.2-17	proximal	13–14	6.15	4.46	1.38

are R-units and not to the distal shield elements. In any case, this new species is included in the genus *Hornibrookina* because it presents the diagnostic characteristics of the genus, in being a narrowly elliptical placolith with a central-area filled by large bars, having a monocyclic proximal shield, and with a bicyclic distal shield with an inner cycle forming a crown-like structure. **Dimensions**: Length = 5.48–6.15 μm; width = 3.66–4.46 μm; axial ratio = 1.34–1.56 (Table 3). **Holotype**: YT.RMP_N.000007.2-10 (Pl. 3, figs 1, 2). **Paratypes**: YT.RMP_N.000007.2-11 (Pl. 3, fig. 3), YT.RMP_N.000007-12 (Pl. 3, fig. 4), YT.RMP_N.000007.2-13 (Pl. 3, fig. 5), YT.RMP_N.000007.2-14 (Pl. 3, fig. 6), YT.RMP_N.000007.2-15 (Pl. 3, fig. 7), YT.RMP_N.000007.2-16 (Pl. 3, fig. 8), YT.RMP_N.000007.2-17 (Pl. 3, fig. 9), YT.RMP_N.000007.1-3 (Pl. 4, figs 1–5), YT.RMP_N.000007.1-4 (Pl. 4, figs 6–15), YT.RMP_N.000007.1-5 (Pl. 4, fig. 16), YT.RMP_N.000007.1-6 (Pl. 4, fig. 17), YT.RMP_N.000007.1-7 (Pl. 4, fig. 18), YT.RMP_N.000007.1-8 (Pl. 4, figs 19, 20), YT.RMP_N.000007.1-9 (Pl. 4, figs 21–24), BAFC-NP 3397-6 (Pl. 4, fig. 25), BAFC-NP 3397-7 (Pl. 4, fig. 26), BAFC-NP 3397-8 (Pl. 4, fig. 27), BAFC-NP 3397-9 (Pl. 4, fig. 28), BAFC-NP 3397-10 (Pl. 4, fig. 29), BAFC-NP 3397-11 (Pl. 4, fig. 30). **Type locality**: Río de la Turba section, Argentina (53.92°S, 68.38°W). **Type level**: Sample 022, La Despedida Group, NP16, Middle Eocene. **Occurrence**: Early to Middle Eocene (NP13–NP16) in the Austral Basin, Patagonia. Late Ypresian to Early Bartonian (NP13–NP16) in the Campo Bola Well (1015–1020 m); Late Lutetian to Early Bartonian (NP16) in the Río de la Turba outcrop.
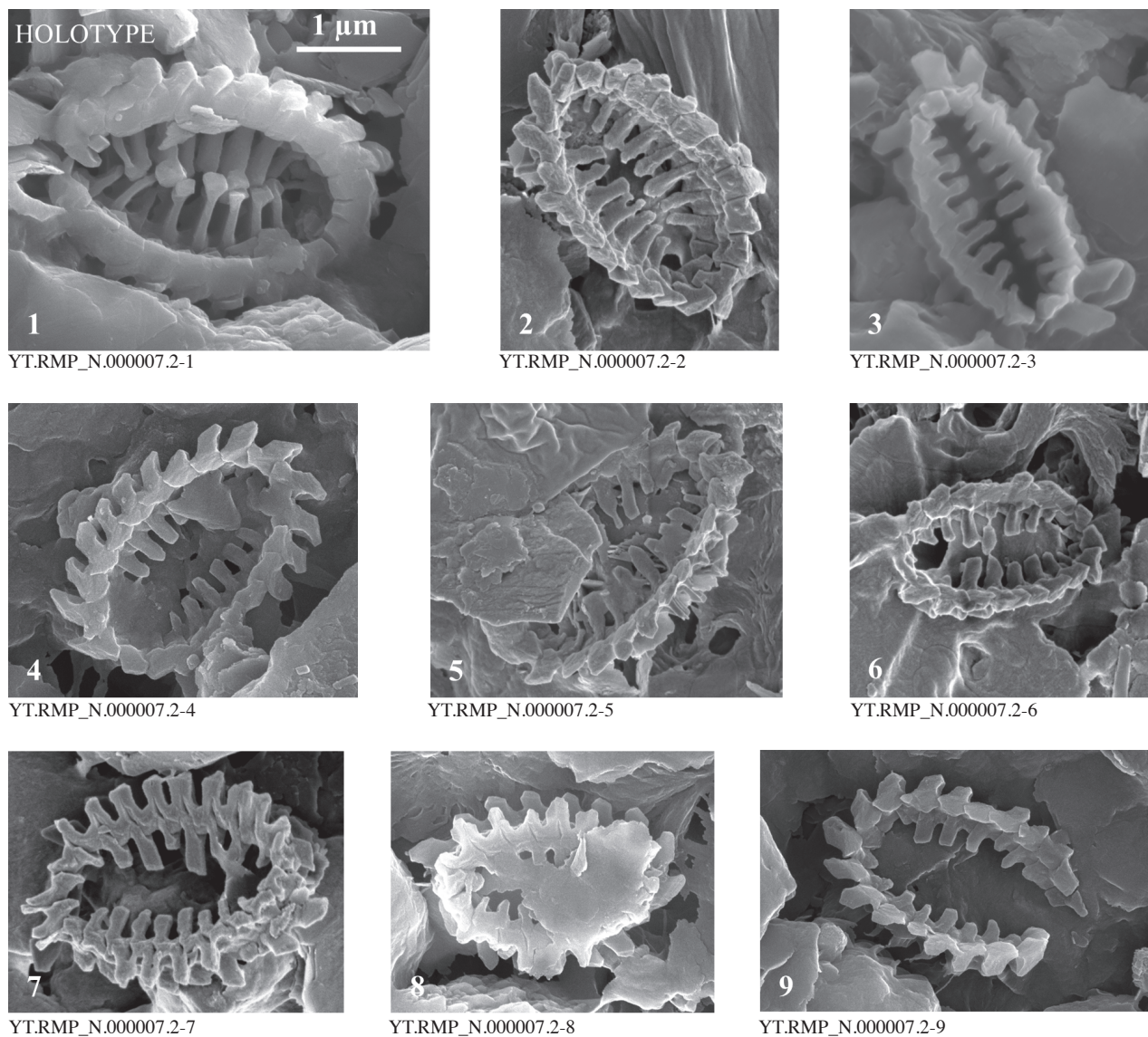
6. Age and palaeoenvironment: Implications for *Hornibrookina* evolution and palaeoecology

Previous foraminiferal analyses of the Río de la Turba outcrop have indicated a Middle Eocene age for this unit (Malumián, 1989, 1990). In terms of nannofossils, based on the co-occurrence of *Sphenolithus predistentus* and

Plate 1

SEM images of *Hornibrookina larae*, Río de la Turba, Sample 022
1: holotype; 2–9: paratypes; 3, 7, 9: proximal views

YT.RMP_N.000007.2-1

YT.RMP_N.000007.2-2

YT.RMP_N.000007.2-3

YT.RMP_N.000007.2-4

YT.RMP_N.000007.2-5

YT.RMP_N.000007.2-6

YT.RMP_N.000007.2-7

YT.RMP_N.000007.2-8

YT.RMP_N.000007.2-9

Reticulofenestra reticulata, which have their base occurrences at or near the base of NP16 of Martini (1971) (see Bown & Dunkley Jones, 2012; Agnini et al., 2014; Raffi et al., 2016), with *Toweius callosus*, which has a top near the NP15/NP16 boundary, we constrained the age of the Río de la Turba outcrop to the Middle Eocene (NP16). The new foraminifera data is in agreement with a Middle Eocene age; the planktonic foraminifera species *Globigerinatheka index* is restricted to the Middle to Late Eocene (Premoli Silva et al. 2006), and its base lies at the E9/E10 biozone boundary of Berggren & Pearson (2005), which coincides

with the base of NP16. The benthic foraminiferal assemblage also supports this age and can be correlated to other known Middle Eocene assemblages in the Austral Basin (Malumián & Jannou, 2010; Malumián & Náñez, 2011).

A comparison of the assemblage from the Río de la Turba section with other Middle Eocene nannofossil assemblages from the Austral Basin revealed some differences in the taxonomic composition and relative abundances (see Pérez Panera, 2009, 2013). The most evident was the absence of the genus *Chiasmolithus*, which is common and diverse in other Middle Eocene assemblag-

Plate 2

LM paratype images of *Hornibrookina larae*
1–5: Río de la Turba, Sample 022;
6–8, 15, 16: Campo Bola, 1015–1020 m; 9–14: Cóndor Oeste, 1065 m

1 µm

1 YT.RMP_N.000007.1-1

2 YT.RMP_N.000007.1-2

3

4

5

6 BAFC-NP 3397-1

7 BAFC-NP 3397-2

8 BAFC-NP 3397-3

9 YT.RMP_N.000009.1-1

10 YT.RMP_N.000009.1-2

11

12

13 YT.RMP_N.000009.1-3

14 YT.RMP_N.000009.1-4

15 BAFC-NP 3397-4

16 BAFC-NP 3397-5
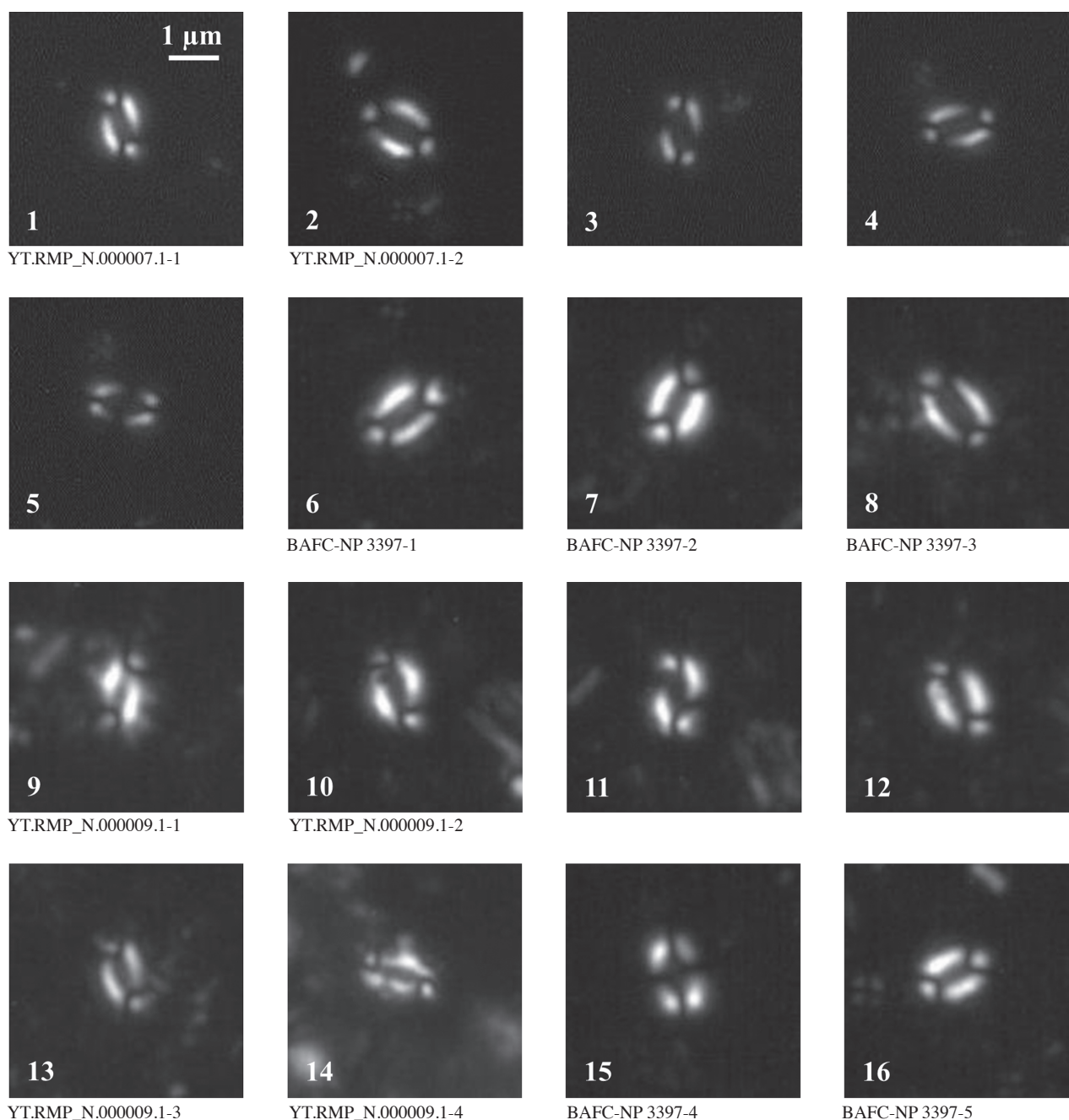
es, the high relative abundance of *Reticulofenestra minuta*, the small size of other reticulofenestrids (see Table 1) and the higher relative abundances of *H. larae* and *H. nicolasii*. The abundance of *Hornibrookina* in the Río de la Turba section is unusually high and most likely related to the palaeoenvironmental conditions. High abundances of small reticulofenestrids and, more specifically, of *R. minuta*, have been associated with high productivity (Pujos, 1985; Gartner, 1992). Moreover, according to Wade & Bown (2006) and Auer et al. (2014), *R. minuta* blooms may have been triggered by enhanced terrigenous nutrient input, generating eutrophic conditions and fluctuating

Plate 3

SEM images of *Hornibrookina nicolasii*, Río de la Turba, Sample 022
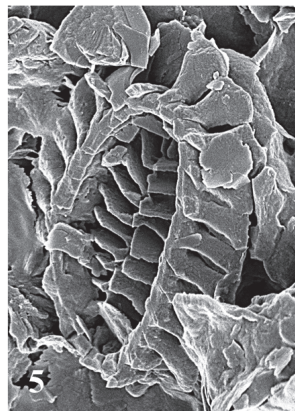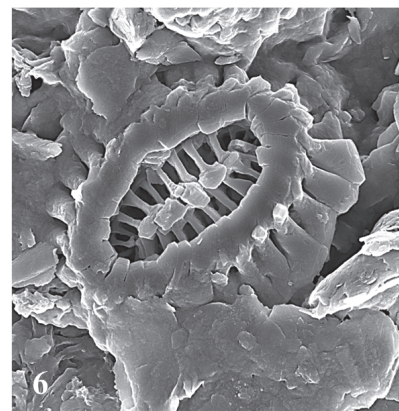1, 2: holotype; 3–9: paratypes; 8, 9: proximal views
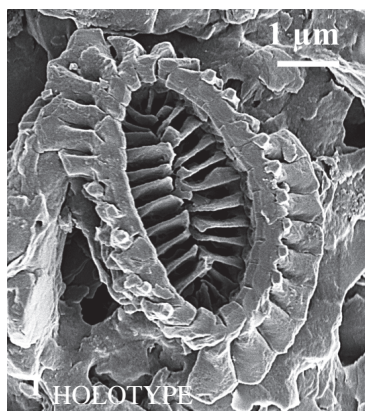
YT.RMP_N.000007.2-10
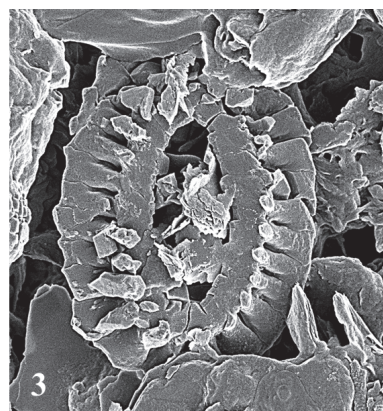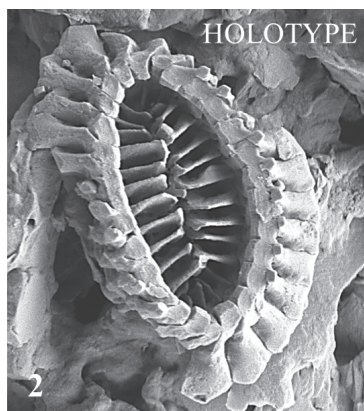
YT.RMP_N.000007.2-11
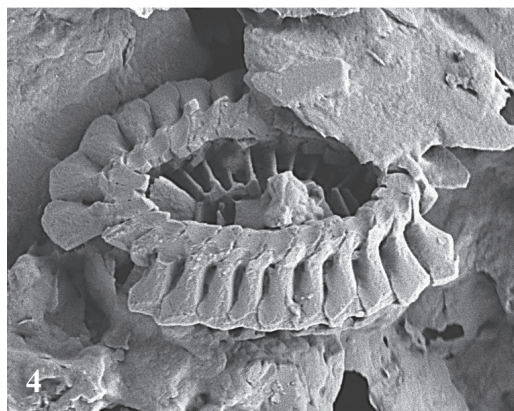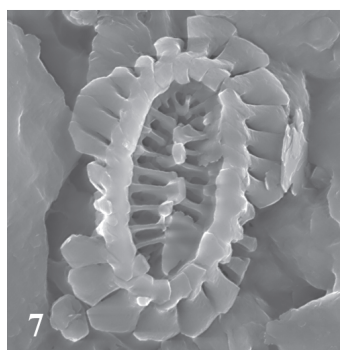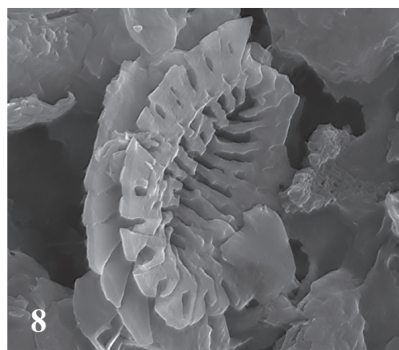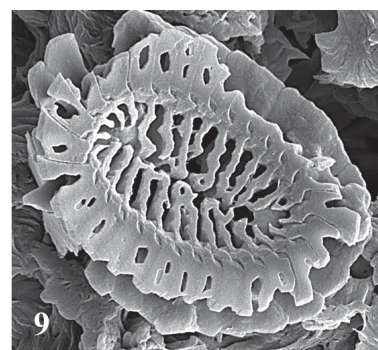
YT.RMP_N.000007.2-12

YT.RMP_N.000007.2-13

YT.RMP_N.000007.2-14

YT.RMP_N.000007.2-15

YT.RMP_N.000007.2-16

YT.RMP_N.000007.2-17

salinity. Schneider et al. (2013) and Leon y Leon et al. (2018) have suggested that the genus *Hornibrookina* had an affinity for coastal, eutrophic surface waters, and the relatively high abundance of these new species in this assemblage supports that palaeoecological interpretation.
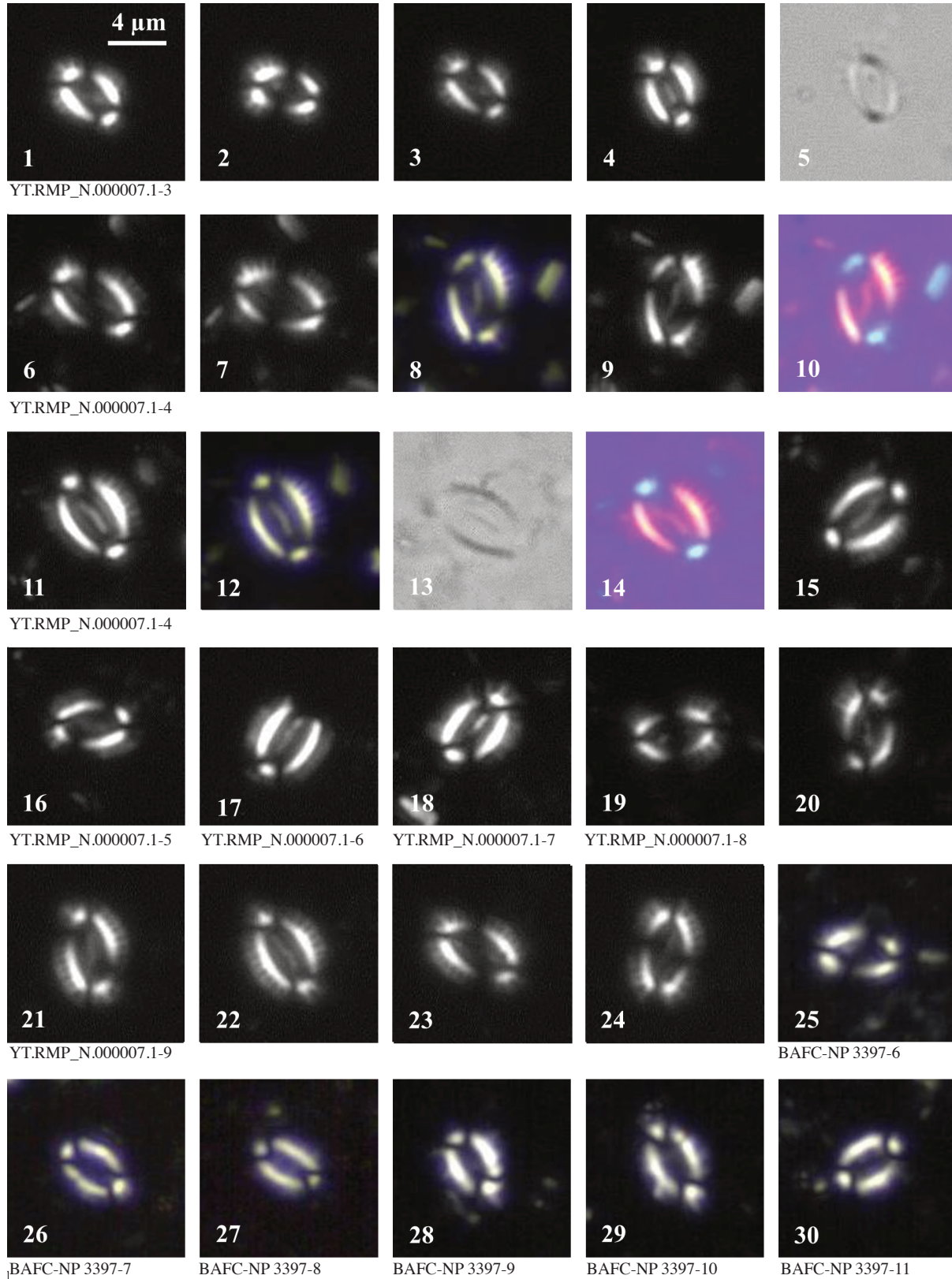
The moderately abundant planktonic and diverse benthic foraminifera might indicate middle- to outer-shelf depths with high-productivity surface waters. Also, a palynological analysis of this sample documented a high abundance of pollen and spores and scarce, poorly preserved dinoflagellate cysts (Pérez Panera et al., 2018). In summary, according to the nannofossil and foraminifera assemblage characteristics, supported by the presence of abundant continental palynomorphs, these sediments were

Plate 4

LM paratype images of *Hornibrookina nicolasii*
1–24: Río de la Turba, Sample 022; 25–30: Campo Bola, 1015–1020 m

YT.RMP_N.000007.1-3

YT.RMP_N.000007.1-4

YT.RMP_N.000007.1-4

YT.RMP_N.000007.1-5   YT.RMP_N.000007.1-6   YT.RMP_N.000007.1-7   YT.RMP_N.000007.1-8

YT.RMP_N.000007.1-9

BAFC-NP 3397-6

BAFC-NP 3397-7   BAFC-NP 3397-8   BAFC-NP 3397-9   BAFC-NP 3397-10   BAFC-NP 3397-11

deposited in ~100–200-m water depths, but relatively close to the coast, and with eutrophic surface waters probably resulting from a high influx of nutrients from continental runoff.

The youngest known occurrence of the genus *Hornibrookina* has been documented by Self-Trail (2011), who recorded *H. arca* just above the base of NP11 (Early Eocene) on the North American shelf. However, Pérez Panera (2013) recorded specimens of what he initially called *H. weimerae* from Early to Middle Eocene cuttings from the Austral Basin. These latter specimens are now considered to be the new species *H. larae*, and a re-examination of the Carpintero, Cóndor Oeste and Campo Bola well samples has revealed the presence of both *H. larae* and *H. nicolasii* from NP13 to NP16. However, a gap in the occurrence of the genus still persists in the Early Eocene of upper NP11 and NP12. The diversity and abundance of this genus diminished across the Paleocene–Eocene transition and during the extreme climate changes of the Early Eocene hyperthermal events, but managed to survive in relict areas, such as the Austral Basin.

7. Conclusions

The two new species—*Hornibrookina larae* and *H. nicolasii*—range from the Early (NP13) to Middle (NP16) Eocene of the Austral Basin, extending the known stratigraphic record of the genus. However, to date, there is no known record of the genus in the NP11–NP12 interval. According to the characteristics of the nannofossil and foraminiferal assemblages in which these new species occurred most abundantly, the coastal and eutrophic affinity of the genus is reinforced.

Acknowledgements

References

Agnini, C., Fornaciari, E., Raffi, I., Catanzariti, R., Pälike, H., Backman, J. & Rio, D. 2014. Biozonation and biochronology of Paleogene calcareous nannofossils from low and middle latitudes. *Newsletters on Stratigraphy*, **47**: 131–181.

Auer, G., Piller, W. & Harzhauser, M. 2014. High-resolution calcareous nannoplankton paleoecology as a proxy for small-scale environmental changes in the Early Miocene. *Marine Micropaleontology*, **111**: 53–65.

Berggren, W.A. & Pearson, P.N. 2005. A revised tropical to subtropical Paleogene planktonic foraminiferal zonation. *Journal of Foraminiferal Research*, **35**: 279–298.

Bown, P.R. & Dunkley Jones, T. 2012. Calcareous nannofossils from the Paleogene equatorial Pacific (IODP Expedition 320 Sites U1331–1334). *Journal of Nannoplankton Research*, **32**: 3–51.

Bramlette, M.N. & Sullivan, F.R. 1961. Coccolithophorids and related nannoplankton of the early Tertiary in California. *Micropaleontology*, **2**: 129–188.

Edwards, A.R. 1973. Key species of New Zealand calcareous nannofossils. *New Zealand Journal of Geology and Geophysics*, **16**: 68–89.

Galeazzi, J.S. 1998. Structural and stratigraphic evolution of the Western Malvinas Basin. *Bulletin of the American Association of Petroleum Geologists*, **82**: 596–636.

Gartner, S. 1992. Miocene nannofossil chronology in the North Atlantic, DSDP Site 608. *Marine Micropaleontology*, **18**: 307–331.

Hay, W.W. & Mohler, H.P. 1967. Calcareous nannoplankton from Early Tertiary rocks at Pont Labau, France and Paleocene–Early Eocene correlations. *Journal of Paleontology*, **41**: 1505–1541.

Leon y Leon, I.A., Bralower, T.B. & Self-Trail, J.M. 2018. Ecological changes in the nannoplankton community across a shelf transect during the onset of the Paleocene–Eocene Thermal Maximum. *Paleoceanography and Paleoclimatology*, **33**: 1396–1407.

Malumián, N. 1989. Foraminíferos bentónicos de la localidad tipo de la Formación La Despedida (Eocene, Isla Grande de Tierra del Fuego). Parte I: Textulariina y Miliolina. *Ameghiniana*, **25**: 341–356.

Malumián, N. 1990. Foraminíferos bentónicos de la localidad tipo de la Formación La Despedida (Eocene, Isla Grande de Tierra del Fuego). Parte II: Nodosariaceae, Buliminaceae, Elphidiidae y rotálidos tuberculados. *Ameghiniana*, **27**: 343–363.

Malumián, N. 1999. La sedimentación y el volcanismo terciarios en la Patagonia extraandina. *In*: R. Caminos (Ed.). *Geología Argentina*. Instituto de Geología y Recursos Minerales. *Anales*, **29**: 557–612.

Malumián, N. 2002. El Terciario Marino. Sus relaciones con el eustatismo. *In*: M.J. Haller (Ed.). *Geología y Recursos Naturales de Santa Cruz*. Congreso Geológico Argentino, No. 15, Relatorio I: 237–244.

Malumián, N. & Jannou, G.E. 2010. Los Andes Fueguinos: El registro micropaleontológico de los mayores acontecimientos paleooceanográficos australes del Campaniano al Mioceno. *Andean Geology*, **37**: 1–30.

Malumián, N. & Náñez, C. 2011. The Late Cretaceous-Cenozoic transgressions in Patagonia and the Fuegian Andes: foraminifera, palaeoecology, and palaeogeography. *Biological Journal of the Linnéan Society*, **103**: 269–288.

Martini, E. 1971. Standard Tertiary and Quaternary calcareous nannoplankton zonation. *In*: A. Farinacci (Ed.). *Proceedings of the II Planktonic Conference*, *Roma*, **2**: 739–785.

Nullo, F.E., Panza, J.L. & Blasco, G. 1999. Jurásico y Cretácico de la Cuenca Austral. *In*: R. Caminos (Ed.). *Geología Argentina*. *Instituto de Geología y Recursos Minerales, Anales*, **29**: 528–535.

Olivero, E.B. & Malumián, N. 2008. Mesozoic–Cenozoic stratigraphy of the Fuegian Andes, Argentina. *Geologica Acta*, **6**: 5–18.

Pascher, A. 1910. Chrysomonaden aus dem Hirschberger Grossteiche. *Monographien und Abhandlungen zur Internationalen Revue der gesamten Hydrobiologie und Hydrographie*, **1**: 66.

Pérez Panera, J.P. 2009. Nanofósiles calcáreos paleógenos del sudeste de la provincia de Santa Cruz, Patagonia, Argentina. *Ameghiniana*, **46**: 273–284.

Pérez Panera, J.P. 2013. Paleogene calcareous nannofossil biostratigraphy for two boreholes in the Eastern Austral Basin, Patagonia, Argentina. *Andean Geology*, **40**: 117–140.

Pérez Panera, J.P., Ronchi, D.I., Hiriart, L. & Ottone, E.G. 2018. *Estudio micropaleontológico en muestras de superficie de la Isla Grande de Tierra del Fuego*. Unpublished Y-TEC Internal Report. Berisso: 35 pp.

Peroni, G., Cagnolatti, M. & Pedrazzini, M. 2002. Cuenca Austral: Marco geológico y reseña histórica de la actividad petrolera. *In*: M. Schiuma, G. Hinterwimmer & G. Vergani (Eds). *Rocas reservorio de las cuencas productivas de la Argentina*. 5ª Congreso de Exploración y Desarrollo de Hidrocarburos, Mar del Plata, 2002. Instituto Argentino del Petróleo y el Gas: 11–20.

Premoli Silva, I., Wade, B.S. & Pearson, P.N. 2006. Taxonomy, biostratigraphy, and phylogeny of *Globigerinatheka* and *Orbulinoides*. *In*: P.N. Pearson, R.K. Olsson, C. Hemleben, B.T. Huber & W.A. Berggren (Eds). *Atlas of Eocene Planktonic Foraminifera*. *Cushman Foundation for Foraminiferal Research, Special Publication*, **41**: 169–212.

Pujos, A. 1985. Late Eocene to Holocene medium- and small-sized "reticulofenestrids". *Proceedings of the INA meeting, Vienna, September 19–22, 1985 (abstracts)*. *INA Newsletter*, **7**: 95–96.

Raffi, I., Agnini, C., Backman, J., Catanzariti, R. & Pälike, H. 2016. A Cenozoic calcareous nannofossil biozonation from low and middle latitudes: A synthesis. *Journal of Nannoplankton Research*, **36**: 121–132.

Sachse, V.F., Strozyk, F., Anka, Z., Rodríguez, J.F. & di Primio, R. 2015. The tectonostratigraphic evolution of the Austral Basin and adjacent areas against the background of Andean tectonics, southern Argentina, South America. *Basin Research*, **28**: 462–482.

Schneider, L.J., Bralower, T.J., Kump, L.R. & Patzkowsky, M.E. 2013. Calcareous nannoplankton ecology and community change across the Paleocene–Eocene Thermal Maximum. *Paleobiology*, **39**: 628–647.

Self-Trail, J. 2011. Paleogene calcareous nannofossils of the South Dover Bridge core, Southern Maryland (USA). *Journal of Nannoplankton Research*, **32**: 1–28.

Wade, B.S. & Bown, P.R. 2006. Calcareous nannofossils in extreme environments: The Messinian salinity crisis, Polemi Basin, Cyprus. *Palaeogeography, Palaeoclimatology, Palaeoecology*, **233**: 271–286.

Young, J.R. & Bown, P.R. 1997. Cenozoic calcareous nannoplankton classification. *Journal of Nannoplankton Research*, **19**: 36–47.